USE OF 3D MEASURING SYSTEM ARAMIS FOR ANALYSIS OF TUBE FLARING PROCESS

EVA PETERKOVA, MARTIN SREFL

Brno University of Technology, Faculty of Mechanical Engineering
Brno, Czech Republic

DOI : 10.17973/MMSJ.2016_11_2016129

e-mail: peterkova@fme.vutbr.cz

This article analyzes the behaviour of a tube sample during the flaring process. The evaluation is carried out using non-contact 3D optical measuring system ARAMIS, which is ranked among the most modern measuring methods of deformations nowadays. The methodology of experiment including the measurement of the required values using GOM Correlate is described in this paper. The stress-strain path of an observed point was created based on the measurement values. The curves of the stress distribution and change of the wall thickness depending on the height of formed tube end were drawn too.

KEYWORDS

tube flaring process, 3D measuring system ARAMIS, stress-strain path

1 INTRODUCTION

Currently, numerical simulation is common help in an area of the metal forming processes. It is employed for analysis of the behaviour of the material during forming process as well as for optimization of the forming process and tools. By use of simulation, a distribution of the stresses and strains, changes of the wall thickness, a capability of metal flow, critical areas and so on, can be predicted. The accuracy of the simulation, however, depends on the correctness of input data such as the corresponding process parameters (coefficient of friction, force, press, ...). Furthermore it depends on an appropriately defined material model, which must be obtained by measuring of the material characteristics. The accuracy of the evaluation is also dependent on appropriately selected simulation parameters such as the mesh size, the integration scheme and other. Alongside numerical simulation, the evaluation of the material behaviour with using the non-contact 3D optical measuring systems is employed for analysis of the forming process in practice too. These measuring systems provide actual and highly accurate results. In comparison with the numerical simulation, their disadvantages are the necessity of an existence of the forming or testing tool and relatively greater time and financial demands. Currently, the main supplier of these systems is the GOM company. The company supplies four measuring systems on the market: ARAMIS, ARGUS, TRITOP Deformation and PONTOS. The second major distributor is the ASAME Technology company. It supplies these systems on the market: GPA and ASAME Model. These 3D optical measuring systems are used largely at the testing departments of the industrial concerns namely for the creation of the idea about the material formability. These systems are often used for obtaining the material characteristics used for numerical simulations too. Furthermore, they can be used for verification of the simulation results of tested samples and for the subsequent optimization of these results. The measuring systems are extensively used for theoretical researches carried out in the laboratories of the research institutes and the universities. This way the important knowledge about the behaviour of different materials during the various ways of the loading are obtained. For example, in sheet metal forming these researches concern the determination of the process limitations in sheet metal forming, the analysis of sheet metal specimens in bulge tests, the determination of material behaviour in tensile tests and others, which are presented by company GOM mbH in [GOM 2010]. 3D photogrammetric system ARGUS was used in the study [Tomas 2015] namely for the measuring of the limit strains on the tinplates. The Nakajima test was used for this investigation. The issue of the non-contact measurement of the limit deformations generated by the above-cited test is also mentioned in [Vollertsen 2013]. An analogous principle of the non-contact 3D optical measurement was used for the analysis of the springback of the bending component in [Zhang 2016]. They have scanned a large number of the significant points at different angles on the made component by use of the surface scanning systems and the photogrammetry and then they have created the cloud of points. The model of the real component was created from these scanned points. This model was subsequently compared with the CAD model of the required shape. Based on this comparing the deviations caused by springback were found out. Currently, there are many other papers regarding the use of these measuring systems. Using this way of measurement it is possible to determine the forming limit curves as well as to analyse the behaviour of the semi-finished product in detail during any way of the loading. In this study the method of the tube flaring is analysed with use of the measuring system ARAMIS.

2 TUBE FLARING PROCES

The tube flaring process is one of the tube end forming methods. The forming of the tube end in the conical shape is realised by pushing the tube onto the conical part of the forming mandrel. The forming mandrel has defined an apical angle 2α and a crossing radius r_m. The motion of tube sample is performed by use the press slide, which pushes on the upper end of the tube, see Fig. 1.

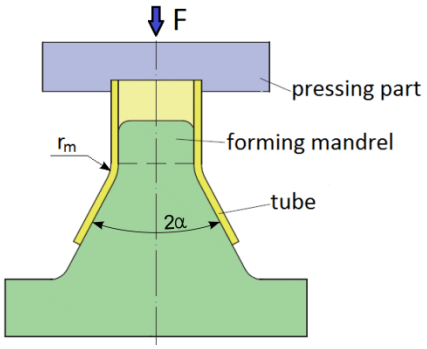

Figure 1. Principle of tube flaring process

At the beginning of the forming process, bending of the tube wall at the radius r_m occurs. At this moment the expanding of the tube is started too. This process takes place in the area between the points 1-2 (Fig. 2). After that, the tube wall only expands and the conical shape occurs. It is the area between points 2 - 3 in Fig. 2.

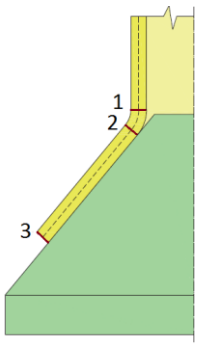

Figure 2. Significant points of formed part

The focus of deformation is situated among points 1-3. According to the theoretical considerations mentioned for example in [Samek 2011], [Gorbunov 1981] the biaxial stress state and three dimensional state of strains occur at this area, see Fig. 3. The theoretical curves of the stress distribution and of the wall thickness changes are shown too, Fig. 3c,d.

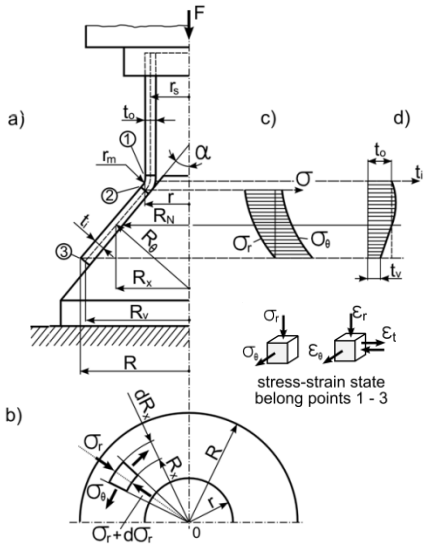

Figure 3. Stress-strain state of tube flaring [Samek 2011]

3 MEASURING SYSTEM ARAMIS

ARAMIS is the optical 3D non-contact measuring system, used especially for measurement of the deformations. It is possible to use this system both for the quasi static loading and for the dynamic loading. The sensor device consists of two CCD cameras and of two LED lights, Fig. 4.

Figure 4. Sensor device

A pair of cameras provides two angles of view, which are necessary for creating of 3D picture. If it is necessary to scan the whole object, it is possible to connect several ARAMIS systems into one. Another advantage of ARAMIS is the possibility to scan a large range of the sizes of components. It is suitable to adapt the camera resolution (respective scan rate) to the measured object and the way of its loading. All data is obtained in real time. The preparation of the samples is very important part in the realization the measurement by using this system. Stochastic pattern of colours is applied to the surface of the samples. This pattern can be seen in Fig. 5.

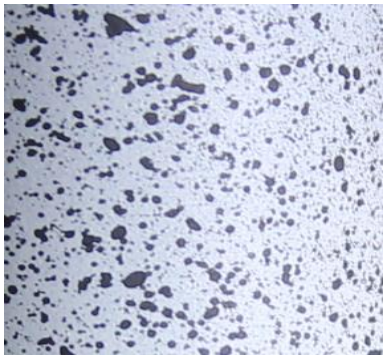

Figure 5. Pattern on surface of samples

The combination of black and white colours is used most frequently. It is important that the ratio of these colours is approximately 50 %. Then the prepared samples are scanned by two CCD cameras. System ARAMIS then divides the observed area into a large number of areas about the size of pixels. And subsequently the ARAMIS will assess so-called gray level in these small areas. It means the unique distribution of black and white colour, for the given area. Points are placed into these areas and their position is determined by using the triangulation method. The points are then connected in a triangular network. The pattern is deformed together with the observed object during the forming process. The loading history is recorded with using two CCD cameras. In the particular levels of deformation the matching points are compared. From this comparison system calculates 3D shifts, shape of deformed object and 3D deformations. The outputs from the measurements are the values of 3D shifts, the data on main and secondary stresses, the changes of the shape in individual phases of the loading, the thick wall changes and the comparing of the deformations with the limit curve (FLC). Measuring system ARAMIS has wide application especially in the following areas:

- the component testing and analysis,
- the optimizing of the forming process (creating FLC),
- the verification and optimization of simulations of metal sheets,
- the detection of areas with a critical deformation,
- the optimizing of the forming tools.

4 EXPERIMENTS

The technological test of the tube flaring was carried out in this study. The aim of this experiment was the creation of an overall picture of the tube´s behaviour during the flaring process using the measuring system ARAMIS and the verifying of the accuracy of the theoretical conclusions created in the past. It primarily concerns the distribution of the stresses and the wall thickness along the formed part of the sample, as it can be seen in Fig. 3. Furthermore the next aim was to obtain the stress-strain path of this forming process.

The stainless steel tube from material 1.4301 was chosen for these experiments. Dimensions of the sample were: outside

diameter D = 28 mm, length L = 85 mm and wall thickness t_0 = 1 mm. After measuring of the wall thickness of the supplied tube it was found out that the real value of the wall thickness is t_0 = 0.86 mm. This measured value was taken into account for the all next analysis. The apical angle was 60 ° and the crossing radius was r_m = 5 mm, Fig. 1. Five samples were tested due to the statistical evaluation. The height of the formed conical part was in accordance with the value of the shift of press slide z = 20 mm. The expanding of the tube end at a cone shape was performed at the tensile testing machine Zwick/Roell Z100 and it was scanned by means of the optical 3D measuring system ARAMIS. The tensile testing machine (1) as well as the CCD cameras (2) were connected to the control computer (3) through which the forming process and the measurement were controlled. The arrangement of the whole device is shown in Fig. 6. The ram speed was chosen 1 mm/sec.

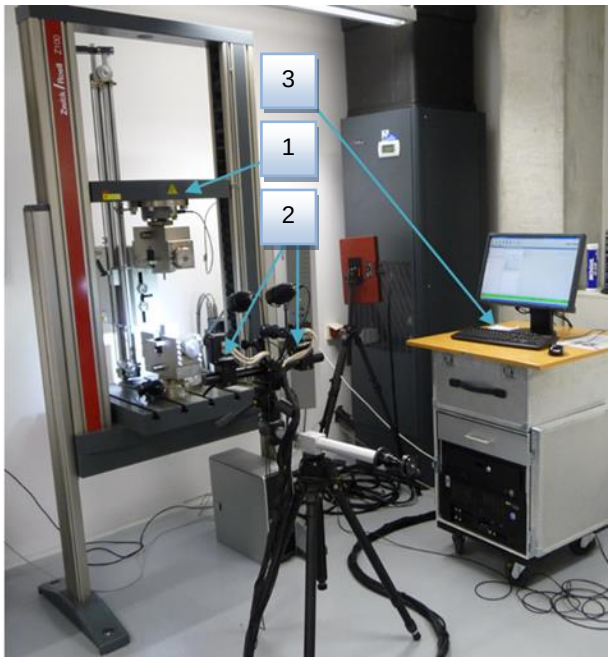

Figure 6. Experimental device

4.1 Preparation of test samples

The first part of the experiment was the application of the stochastic pattern on the surface of the samples. The samples were placed into the exhausting chamber. At first the white matt paint was sprayed on the samples, as can be seen in Fig. 7.

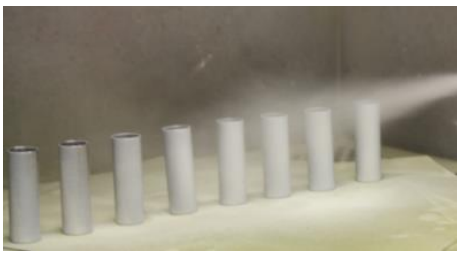

Figure 7. Experimental device

The small stains of the black paint were created after the drying of the white paint. These spots were created by squeezing the spray with a black paint very gently. The black paint was applied from the distance of 400 mm. The samples with applied pattern are shown in Fig. 8.

Figure 8. Samples with applied pattern

The measured data were processed in the GOM Correlate programme. At first the CAD model of the tube was added to the scanned area and then this scanned area was supplied with the coordinate system, wherein the z-axis is identical with the axis of the tube, Fig. 9.

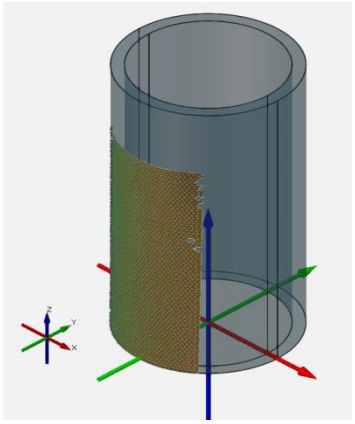

Figure 9. The investigated area of tube

The values of forming forces and the displacements of ram were written during this forming process. Subsequently, the work curve F= f(z) was created from these values. The graph of this relationship is shown in Fig. 10.

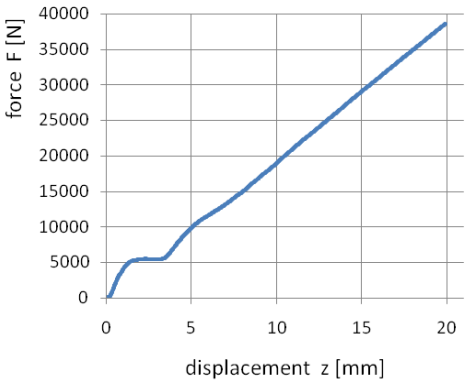

Figure 10. Work curve F = f(z)

Using the program GOM Correlate it is possible to evaluate a wide range of the quantities such as the proportional deformations ε, the wall thinning, 3D displacement of a point and the like. These values can be determined for any point located in the monitored area of the tube which is shown in Fig. 11.

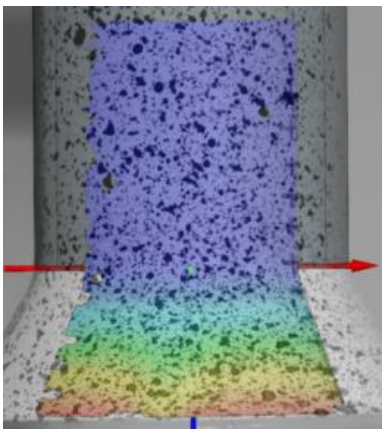

Figure 11. Monitored area of sample

Evaluation of wall thickness distribution

The values of the wall thickness were determined at selected points which were regularly distributed along the height of the deformed part of the sample. Using the program GOM Correlate the cross-sections having the shape of the circle of radius R_x were created in these points, (Fig. 3) or (Fig. 15). For a better definition of the various heights in this program the zero value of height was chosen approximately 1 mm from the beginning of the crossing radius r_m, see Fig. 12. The distance between the individual cross-sections was 1 mm. This distance (step) has been reduced to 0.5 mm at the area of the bend and at the edge of the sample. This was done for a better evaluation of the behaviour of the material at these critical places.

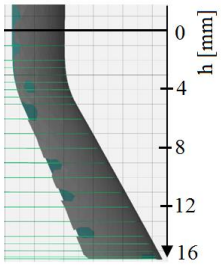

Figure 12. Dividing of the height at the individual steps

After determination of the values of the real wall thickness at individual cross-sections the curve of the dependence of the wall thickness on the height of the deformed part was created. This relationship is shown in Fig. 13.

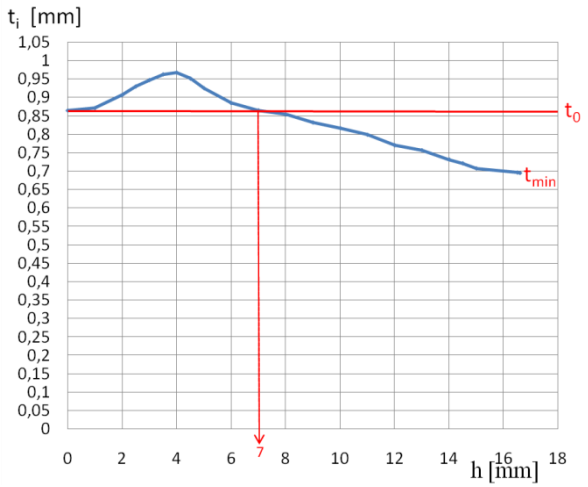

Figure 13. Graph of relationship $t_i = f(h)$

The Fig. 13 shows that the wall thickness increases in the bending area and slightly behind it. So-called upsetting of the wall thickness occurs here. However, for the analyzed samples the value of the wall thickness is again equal to the initial value t_0 in the distance of about 7 mm from the approximate beginning of the bending. Radius, on which the initial value of the wall thickness is situated, is called the neutral radius R_N, see Fig. 3. After the crossing of this value the wall thinning occurs approximately in linear relationship. The minimum value of the wall thickness (t_{min} = 0.69 mm) is achieved at the edge of the tube. Better said, it occurs in the place of the maximum tube extension of the radius R_v. By comparing the curves of the wall thickness change in Fig. 13 and in Fig. 3, it can be concluded that these curves are almost identical. Moreover, Fig. 13 is a benefit, because, unlike Fig. 3, it describes the area of the bend between points 1 and 2. The distribution of the wall thickness along the height of the investigated area can be viewed using program GOM Correlate. Here the dark blue colour represents the maximum of the wall thickness increase and vice versa, the red colour represents the maximum of the wall thinning, see Fig. 14.

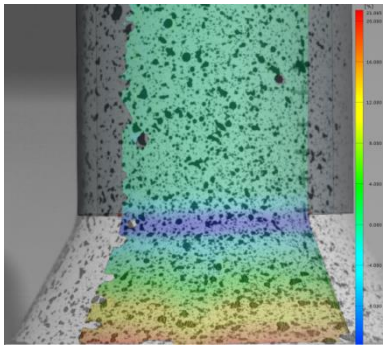

Figure 14. Colour map of wall thickness change

Stress state

The biaxial stress state is considered at the focus of deformation (among points 1 - 3, Fig. 3) during the tube flaring process. There are the deformation stress in the circumferential direction σ_θ and the deformation stress in the radial (meridional) direction σ_r. The values of these main stresses can be calculated with using theoretical equations derived for example in [Samek 2011], [Gorbunov 1981] for the individual cross-sections (heights) of the sample´s deformed part.
The equation for the radial stress has form:

$$\sigma_r = -\sigma_k \cdot \left(1 + \frac{\tan(\alpha)}{\mu}\right) \cdot \left[1 - \left(\frac{R_x}{R_v}\right)^{\mu \cdot \cot(\alpha)}\right] \quad (1)$$

The circumferential stress can be expressed as:

$$\sigma_\theta = \sigma_k \cdot \left\{1 - \left(1 + \frac{\tan(\alpha)}{\mu}\right) \cdot \left[1 - \left(\frac{R_x}{R_v}\right)^{\mu \cdot \cot(\alpha)}\right]\right\} \quad (2)$$

where σ_k is yield stress [MPa], μ is coefficient of friction [-], α is apical angle of the cone [°], R_x is radius of the circle of the selected cross-section [mm], see Fig. 15, R_v is radius of the maximal tube extension [mm]. For calculations the values σ_k = 385 MPa and μ = 0.15 were used.

After calculation of the main stresses at individual cross-sections the curves of the stress distribution along the height of the deformed part can be drawn. The stress-versus-height relationship σ_r, $\sigma_\theta = f(h)$ is shown in Fig. 16.

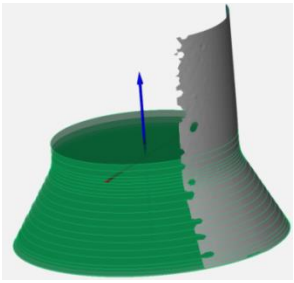

Figure 15. Cross-sections corresponding with chosen heights

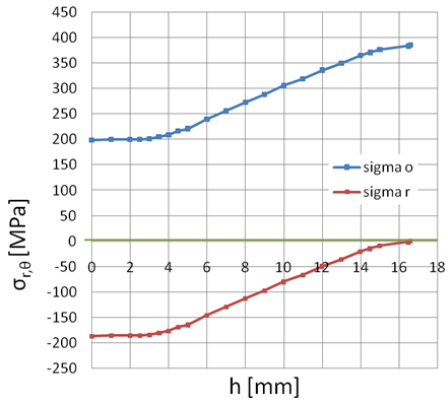

Figure 16. Relationship σ_r, σ_θ = f(h)

From the curve of the radial stress distribution it can be concluded that this stress has pressure character (it is negative) and its maximum value is situated at the point of zero height h = 0 mm. In other words, $(\sigma_r)_{max}$ is located at the beginning of the deformed part, above the crossing radius r_m. With increasing value of the radius of the conical part, the value σ_r is falling to almost zero. The other way around, circumferential stress has minimum value at the point of h = 0 mm and maximum value at the edge of sample, at the place of the maximal tube extension. This is proof that only tensile circumferential stress acts at the edge of the cone. The uniaxial tension occurs at the radius R_v.

Stress-strain path

Regarding stress and strain, the material behaviour during the forming process can be expressed by the so-called stress deformation path. In this case it is necessary to watch the change of the stress-strain at one selected point of the sample namely during the whole forming process. It can be easily done using program GOM Correlate, because this program is able to determine the values at any time and for any point belonging investigated area. In this study, the stress-strain path was analysed for a selected point on the edge of the tube. The shift of the selected point during the forming process is shown in Fig. 17.

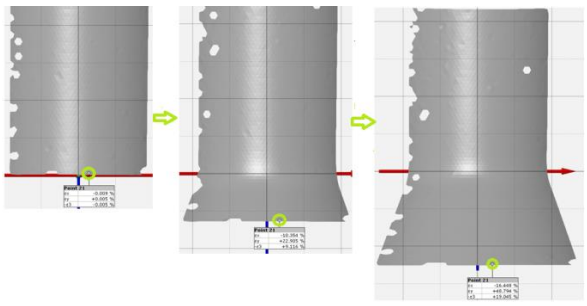

Figure 17. Shift of selected point

The values of the deformations ε_r, ε_θ in different directions and their corresponding radius R_x were found out for a pre-defined positions of the investigated point. These positions correspond with the cross-sections in Fig. 15. By using Eq. (1) and Eq. (2) the values of the main stresses σ_r a σ_θ were calculated, as well as a value of effective stress σ_{ef} for biaxial stress state. The following equation for the effective stress was used to calculate [Forejt 2006].

$$\sigma_{ef} = \sqrt{\sigma_r{}^2 - \sigma_r \cdot \sigma_\theta + \sigma_\theta{}^2} \tag{3}$$

Furthermore the values of the effective deformations φ_{ef} were determined. The known relations were used [Forejt 2006]:

$$\varphi_{ef} = \frac{\sqrt{2}}{3}\sqrt{(\varphi_r - \varphi_\theta)^2 + (\varphi_\theta - \varphi_t)^2 + (\varphi_t - \varphi_r)^2} \tag{4}$$

where logarithmic values of the deformations were determined by the following equations:

$$\varphi_r = \ln(1 - \varepsilon_r) \tag{5}$$

$$\varphi_\theta = \ln(1 + \varepsilon_\theta) \tag{6}$$

And from volume conservation law then:

$$\varphi_t = -(\varphi_r + \varphi_\theta) \tag{7}$$

The curve of relationship σ_{ef} = f(φ_{ef}) based on calculated effective values of stress and strain was plotted, Fig. 18. This curve can be considered as the stress-strain path.

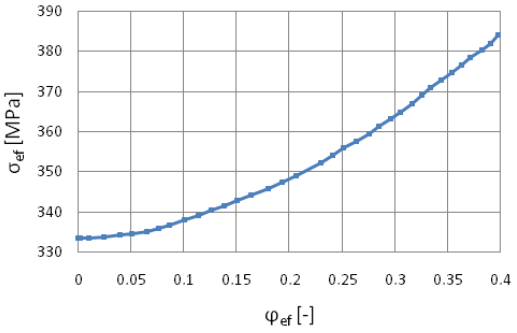

Figure 18. Stress-strain path

5 CONCLUSIONS

In this study, the analysis of the tube flaring process by using 3D optical measurement system ARAMIS was carried out. On the basis of the measured values the curves of the stresses distribution and the wall thickness change in dependence on height of the deformed part of the sample were plotted. The created curves correspond with the curves presented in theories concerning the same forming process. Their accuracy was confirmed in this way. Thanks to this study, the theoretical curves were enriched by adding the curve of the relationship of the effective stresses and strains, so called the stress-strain path. By using the measuring system ARAMIS it was possible to create real idea about the behaviour of tube during the tube flaring process. Many other graphs can be created using the system ARAMIS and program GOM Correlate such as stresses-maximal radius of cone relationship, wall thickness-maximal radius of cone, the plotted points in the forming limit diagram and more. In conclusion it can be said, the non-contact 3D

measuring optical systems are great benefit in the sheet metal forming and together with the numerical simulation it holds an important position in the field of the analysis of the forming processes and the designing of the optimal forming tools.

ACKNOWLEDGMENTS

This paper was elaborated with the support of specific research Faculty of Mechanical Engineering, Brno University of Technology relating to the grant no. FSI-S-14-2394. Thanks belong to MCAE Systems, s.r.o. company for the realization of experiments and valuable advices in their evaluation.

REFERENCES

[Forejt 2006] Forejt, M. and Piska, M. Theory of Machining, Forming and Tools. Brno: Academic Publishing CERM, 2006. ISBN 80-214-2374-9 (in Czech).

[Gom 2010] GOM mbH. Optical Measuring Techniques. 2016, Germany [online]. [16-08-15] Available from <http://www.gom.com/>.

[Gorbunov 1981] Gorbunov, M.N. Technology of Sheet Metal Forming in Aircraft Manufacturing. Moskva: Mašinostrojenije, 1981. (in Russia)

[Samek 2011] Samek, R., et al. Special Forming Technology - Part II. Brno: Academic Publishing CERM, 2011. ISBN 978-80-214-4406-5 (in Czech).

[Srefl 2016] Srefl, M. Flaring the end of the tube under static and dynamic conditions, Master´s Thesis http://hdl.handle.net/11012/60868. Brno: Brno University of Technology, Faculty of Mechanical Engineering, Institute of Manufacturing Technology, 2016 (in Czech).

[Tomas 2015] Tomas, M., et al. Measurement of the Limit Strains on TS 245 Tinplate. Materials Science Forum, 2015, Vol. 818, pp 213-216. ISSN: 1662-9752.

[Vollertsen 2013] Vollertsen, F., Micro Metal Forming. Berlin: Springer-Verlag Berlin Heidelberg, 2013. ISBN 978-3-642-30916-8.

[Zhang 2016] Zhang, D., et al. A novel 3D optical method for measuring and evaluating springback in sheet metal forming process. Measurement, 2016, Vol. 92, pp 303-317. ISSN 0263-2241.

CONTACTS

Ing. Eva Peterkova, Ph.D.
Brno University of Technology
Faculty of Mechanical Engineering
Department of Metal Forming
Technicka 2896/2, 616 69 Brno, Czech Republic
Tel.: +420 54114 2637
e-mail: peterkova@fme.vutbr.cz

Ing. Martin Srefl
Brno University of Technology
Faculty of Mechanical Engineering
Department of Metal Forming
Technicka 2896/2, 616 69 Brno, Czech Republic